X-ray Study of Lattice Tensile Properties of Fully Extended Aromatic Polyamide Fibers over a Wide Temperature Range

Tadaoki Ii,† Kohji Tashiro, Masamichi Kobayashi,* and Hiroyuki Tadokoro

Department of Macromolecular Science, Faculty of Science, Osaka University, Toyonaka, Osaka 560, Japan. *Received February 18, 1986*

ABSTRACT: X-ray diffraction has been used to measure the lattice strain ϵ_l along the chain axis as a function of temperature and tensile stress for highly oriented poly(*p*-benzamide) (PBA) and poly(*p*-phenyleneterephthalamide) (PPTA) fibers. $\epsilon_l(T)$ shows a smooth and reversible thermal contraction; the thermal expansion coefficient has been estimated as -6.7×10^{-6} K^{-1} for PBA and as -3.4×10^{-6} K^{-1} for PPTA under a tensile stress of 0.05 GPa in the temperature range 300–600 K. The compliance $J_l(T)$ is 5.3×10^{-3} GPa^{-1} for PBA and 6.0×10^{-3} GPa^{-1} for PPTA at 293 K and it increases gradually with a rise of temperature; $\Delta J_l/\Delta T$ is 7.1×10^{-6} (GPa·K)$^{-1}$ for PBA and 6.4×10^{-6} (GPa·K)$^{-1}$ for PPTA in the range 300–600 K. These temperature dependences have been interpreted consistently in terms of thermal fluctuations occurring perpendicularly to the chain axis. The lattice modulus extrapolated to 0 K is 235 GPa for PBA and 200 GPa for PPTA, whose values are in good agreement with the theoretical moduli reported by several investigators. All these lattice data have been compared with macroscopic tensile property data to elucidate the characteristic morphological features of these fibers.

Introduction

The highly oriented fibers of poly(*p*-benzamide) (PBA) and poly(*p*-phenyleneterephthalamide) (PPTA) are well-known to show unusually high moduli and to be composed of fully extended molecular chains.[1–8] Even in the noncrystalline phase, the chain is considered to be highly uniaxially arrayed with poor lateral order (paracrystalline structure).[9,10] Therefore these polymer fibers are considered to be the most suitable materials to investigate the thermal and mechanical properties of the fully extended chains, one of the typical aggregate phases of polymers.

It is already known that for many polymers the thermal expansion coefficient along the fiber axis exhibits a small, negative value.[11–13] Such a thermal contraction of the chain has been ascribed to thermal fluctuations of the molecular chain occurring perpendicularly to the chain axis (torsional vibration[12,13] or lateral motions[14] of the molecular chain) at a finite temperature. In a previous paper[15] we observed a reversible and smooth contraction along the fiber direction with a rise of temperature for annealed PBA and PPTA fibers by using thermomechanical analysis. In another paper[16] we found a similar thermal contraction for the *c* axis of PBA and PPTA crystals based on X-ray diffraction. The fairly good parallel relationship in the thermal contraction between the bulk and the crystal lattice has been ascribed to the common origin of the above-mentioned thermal fluctuation mechanism of the fully extended molecular structure.

The crystal lattice modulus along the chain axis is an important guide for the limiting value of the macroscopic modulus along the fiber direction. As stated above, the thermal contraction or thermal expansion occurs at a finite temperature more or less as a result of the thermal agitation. Thus it seems an important problem to estimate how the thermal vibration affects the crystalline modulus. A few investigators[17–19] have reported a temperature dependence of the lattice modulus along the chain axis based on X-ray diffraction. They attributed this dependence to a morphological effect (e.g., a modulus variation in the amorphous part)[17] or interpreted it as being a result of the specific properties of the individual polymers.[18,19] Such a temperature dependence of the crystalline modulus, however, has not yet been discussed as a general property of the polymer lattice itself. In previous papers,[15,20] we observed a smooth increase in compliance with a rise of temperature for PBA and PPTA fibers by the ultrasonic and tensile testing methods (for convenience, the compliance, i.e., the inverse of modulus, has been mostly used in a series of our papers to compare the experimental results with the theoretical results more intimately). This increase in *macroscopic compliance* has also been assumed to originate from a slight contraction of the fully extended chain caused by the thermal agitation. In order to verify the validity of this assumption, a similar increase should be observed, first of all, in *lattice compliance*.

In this paper, we will show the stress dependence of the lattice strain along the chain axis at various temperatures for PBA and PPTA based on X-ray measurements, from which the lattice contraction and the lattice compliance will be derived as a function of temperature. We will also try to clarify the morphological features of these fibers by comparing the temperature dependences of the contraction and compliance for the lattice with those for the bulk.

Experimental Section

Materials. Two sorts of ultrahigh-modulus aramide fibers produced by Du Pont have been examined, namely, PRD 49 for PBA and Kevlar 49 for PPTA.[21] The density ρ of the fiber is 1.483 g/cm^3 for PRD 49 and 1.485 g/cm^3 for Kevlar 49 at room temperature.[15] PBA belongs to the orthorhombic system[22] with a = 0.771 nm, b = 0.514 nm, c (fiber axis) = 1.28 nm, N (number of chains per unit cell) = 2, and ρ_c (the crystal density) = 1.54 g/cm^3. PPTA belongs to the monoclinic system[22,23] with a = 0.780 nm, b = 0.519 nm, c (fiber axis) = 1.29 nm, N = 2, and ρ_c = 1.50 g/cm^3.[22] (Other data for the crystal density: ρ_c = 1.48 and 1.53–1.54 g/cm^3.[23])

X-ray Diffraction Measurement under Tensile Stress. Figure 1 illustrates the X-ray diffraction measuring system equipped with a stress loading instrument and a thermocontrolled cell. Ni-filtered Cu Kα radiation (λ = 0.1542 nm) was used as an X-ray source. The diffracted beams were detected by a position-sensitive proportional counter (PSPC) (3), which was set 30 cm from the sample position. The bundle of filaments (2) was set in the cell (8) horizontally. One end of the bundle was fixed on a load cell (5), and each filament of the bundle at the other end was slightly tightened and wound on a sharp notch cut on one of the pulleys (6). The load F acting on the fiber sample was intensified about 10 times the original weight (7) positioned above the center of the turntable (4) by the set of pulleys. The cross-sectional area of the sample S and the tensile stress σ_t were calculated as

$$S = w/(l\rho) \quad (1)$$

$$\sigma_t = F/S \quad (2)$$

† Current address: Polymer Laboratory, Corporate Research Institute, Sekisui Chemical, Shimamoto, Mishima, Osaka 618, Japan.

0024-9297/87/2220-0347$01.50/0

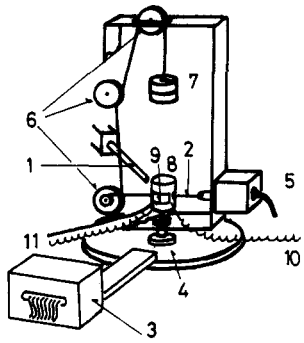

Figure 1. X-ray measuring system equipped with a stress loading instrument and thermocontrolled cell: (1) collimator of X-ray beams; (2) fiber sample; (3) PSPC detector; (4) turntable; (5) load cell; (6) pulley; (7) weight; (8) thermocontrolled cell; (9) aluminum foil window; (10) CA thermocouple (for temperature detection); (11) heater and CA thermocouple (for thermocontrolling).

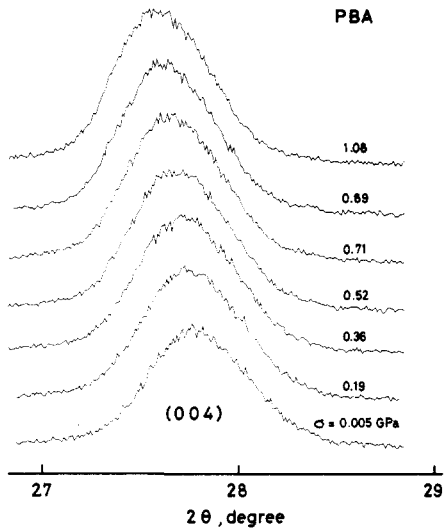

Figure 2. Stress dependence of the X-ray (004) reflection for as-received PBA at room temperature.

where w and l are the mass and length of the fiber sample.

Figure 2 shows a typical example of the stress dependence of the (004) reflection for the as-received PBA sample at room temperature. The lattice strain of the c axis was calculated by

$$\epsilon_l = -\frac{1}{2} \cot \theta \, \Delta(2\theta) \tag{3}$$

where $\Delta(2\theta)$ is the shift in Bragg angle at the peak position under an applied stress at a measuring temperature. A positive (negative) value of ϵ_l means a lattice elongation (contraction). Before X-ray measurement, all samples were annealed under a tensile load for about 15 min in order to eliminate effects of thermal history. X-ray measurement was carried out at temperatures between 300 and 600 K.

Definitions of the Crystalline, Lattice, and Tensile Moduli and the Corresponding Compliances. In the measurement of the crystal lattice modulus by X-ray diffraction, it has been assumed that the stress σ_l acting in the crystalline part is equal to the applied bulk stress σ_t (series model).[24,25] In keeping with this assumption, we define three different quasi-static moduli along the fiber direction (eq 4–6) and the corresponding compliances (eq 7).

(true) crystalline modulus $E_c = \partial\sigma_l/\partial\epsilon_l$ (4)

lattice modulus $E_l = \partial\sigma_t/\partial\epsilon_l$ (5)

(bulk) tensile modulus $E_t = \partial\sigma_t/\partial\epsilon_t$ (6)

compliance (i = c, l, t) $J_i = 1/E_i$ (7)

ϵ_l and ϵ_t denote the lattice strain along the chain axis and the macroscopic strain along the fiber direction, respectively. The values of the strains ϵ_l and ϵ_t and the stress σ_t were calculated from the original sample length, cell dimension, and cross-sectional area at room temperature, irrespective of the measuring temperature (see eq 1–3). From these values the E_i or J_i (i = l, t) were determined on the basis of eq 5–7. Thus they correspond to the values per original cross-sectional area at room temperature, which contains a constant number of molecular chains. Such definitions seem more convenient to discuss the temperature dependence of E_i or J_i from the viewpoint of molecular theory and are consistent with the definition of sonic compliance in the previous paper.[15] In this paper we use the term "macroscopic modulus" as a general term for the tensile, dynamic, and sonic moduli and so on for the bulk sample along the fiber direction.

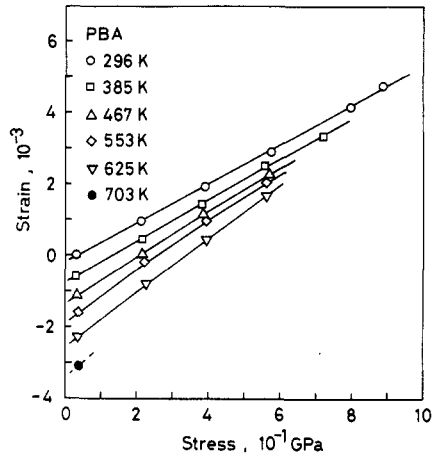

Figure 3. Stress and temperature dependences of the c-axis strain for annealed PBA. Annealing conditions: 0.56 GPa, 625 K, and 15 min. The lattice spacing at room temperature under the smallest stress was taken as an initial standard value for calculating the strain.

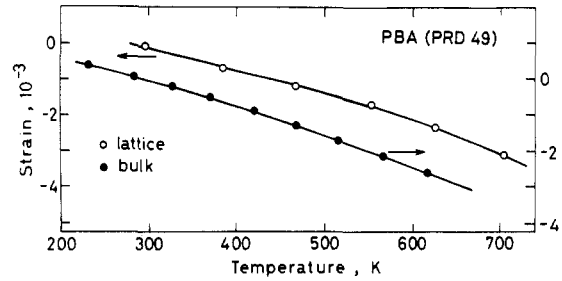

Figure 4. Temperature-dependences of lattice and bulk strains at σ_t = 0.05 GPa for annealed PBA.

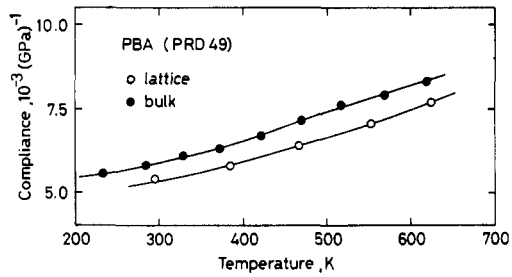

Figure 5. Temperature dependences of compliance of the lattice (between σ_t = 0.02 GPa and σ_t = 0.4 GPa) and bulk (at σ_t = 0.15 GPa) for annealed PBA.

Results and Discussion

PBA. In Figure 3 is plotted the lattice strain ϵ_l against the tensile stress σ_t at various temperatures. The compliance can be obtained from the slope of the strain–stress curve at each temperature. The temperature dependence of the strain is estimated by reading out the value of the strain at a certain stress σ_t = 0.05 GPa. In Figures 4 and 5 $\epsilon_l(T)$ and $J_l(T)$ (open circles) are compared with the bulk strain $\epsilon_t(T)$ and the bulk tensile compliance $J_t(T)$ (closed

Table I
Comparison of Moduli Obtained by Various Methods for PBA

Experimental Moduli (GPa)

	present authors[a]	Slutsker et al.[8]
lattice	188	182
tensile	171[b]	157
sonic	185[c]	167

Theoretical Moduli (GPa)

	Fielding-Russell[26]	Tadokoro et al.[6]	Perepelkin et al.[27]
trans conf	200	238	232
cis conf		163	178

[a] Modulus at 293 K for annealed PBA (PRD 49). [b] Under σ_t = 0.15 GPa. [c] Under σ = 0.109 GPa.

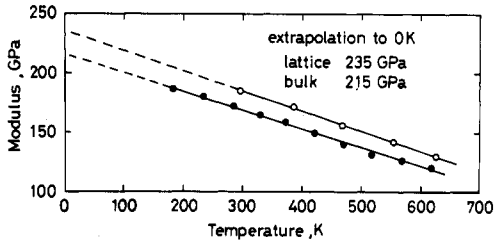

Figure 6. Temperature dependences of modulus of the lattice and bulk for annealed PBA with their extrapolation to 0 K.

circles), respectively. These bulk data have been obtained from macroscopic tensile testings at various temperatures, which have already been reported.[20]

In Figure 4, the curves show thermal contraction behavior of the lattice and bulk for PBA. The averaged thermal expansion coefficients in the temperature range 300–600 K under the stress 0.05 GPa are estimated as -6.7×10^{-6} K^{-1} for the lattice and -8.1×10^{-6} K^{-1} for the bulk. In Figure 5, $J_l(T)$ increases smoothly and gradually with a rise of temperature, similarly to $J_t(T)$; this increase is estimated as 40% from 300 to 600 K for both the lattice and the bulk. The increase in lattice compliance with temperature is just the phenomenon expected to result from the thermal fluctuation of the molecular chain in the crystalline region.

For comparison of these data with those by other workers[8,26,27] and us,[6] it is convenient to rewrite such data as the modulus. In Table I are listed several literature values of the modulus E for PBA, together with ours. The experimentally obtained moduli by Slutsker et al.[8] are similar to ours, suggesting that the morphology of the PBA sample examined by them is similar to ours (PRD 49). The theoretical modulus should be compared with the lattice modulus estimated at 0 K because the lowering of the lattice modulus occurs at a finite temperature due to the thermal agitation. In Figure 6 are plotted the data of E vs. T for the lattice and bulk; the data fit a straight line better than the case of J vs. T shown in Figure 5. Thus the linear extrapolation to 0 K has been tried for the E vs. T curves. The extrapolated lattice modulus 235 GPa is approximately equal to the higher values in the theoretical estimation listed in Table I.

PPTA. Figure 7 shows the ϵ_l vs. σ_t relation at various temperatures for the PPTA fiber. The measurements in the higher stress range were tried up to a high temperature but sufficient data could not be collected, because breakdown of the fiber bundle occurred frequently during the experiment. In the case of PBA (Figure 3), each ϵ_l vs. σ_t curve fits a slightly convex curve with $\partial^2\epsilon_l/\partial\sigma^2 = \partial J_l/\partial\sigma < 0$. As for PPTA, however, the curves for 300 K and 407

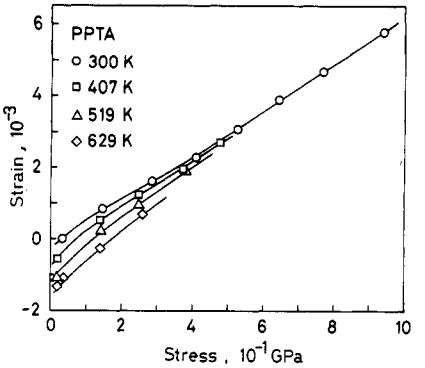

Figure 7. Stress and temperature dependences of the c-axis strain for annealed PPTA. Annealing conditions: 0.26 GPa, 629 K, and 15 min. The lattice spacing at room temperature under the smallest stress was taken as an initial standard value for calculating the strain.

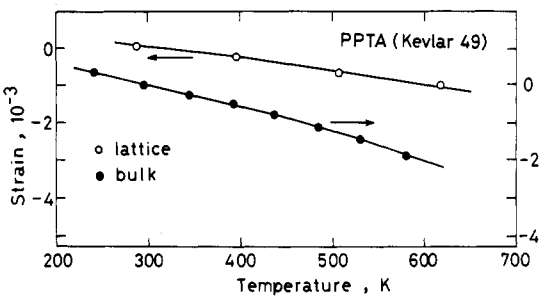

Figure 8. Temperature dependences of the lattice and bulk strains at σ_t = 0.05 GPa for annealed PPTA.

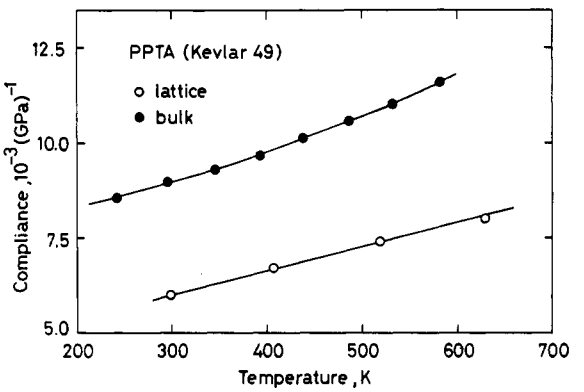

Figure 9. Temperature dependences of compliance of the lattice (between σ_t = 0.1 GPa and σ_t = 0.4 GPa) and bulk (at σ_t = 0.15 GPa) for annealed PPTA.

K do not fit such a simple curve but show a rather complex shape around σ_t = 0.3 GPa. Such a characteristic behavior of the curve is reversible for the cyclic loading and unloading process and has been also observed for the as-received PPTA sample. At the present stage, however, the reason for this phenomenon detected for the crystal lattice of PPTA is not yet obvious.

In Figures 8 and 9, $\epsilon_l(T)$ and $J_l(T)$ (open circles) obtained from Figure 7 are compared with $\epsilon_t(T)$ and $J_t(T)$ (closed circles), respectively. Different from the case of PBA shown in Figures 4 and 5, considerable differences between the lattice and macroscopic values are recognized in these figures. Such a large difference was also present in the modulus data of Slutsker et al.[8] and Gaymans et al.,[7] which are listed in Table II. Figure 10 shows the temperature dependences of lattice and tensile moduli. The extrapolated values to 0 K (broken lines) are about 200 GPa (lattice modulus) and about 138 GPa (tensile modulus). The extrapolated lattice modulus is in satisfactory agree-

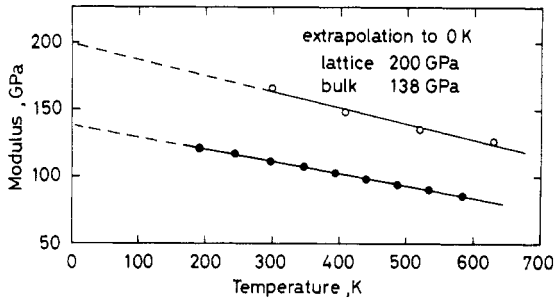

Figure 10. Temperature dependences of modulus of the lattice and bulk for annealed PPTA with their extrapolation to 0 K.

Table II
Comparison of Moduli Obtained by Various Methods for PPTA

Experimental Moduli (GPa)

	present authors[a]	Slutsker et al.[8]	Northolt et al.[10]	Gaymans et al.[7]	Kaji and Sakurada[28]
lattice	168	182	112	200	153
tensile	112[b]	88	105[d]	110[d]	
sonic	147[c]	121	103[e]		

Theoretical Moduli (GPa)

	Fielding–Russel[26]	Tadokoro et al.[6]	Perepelkin et al.[27]
trans conf	200	182	232
cis conf			178

[a] Modulus at 293 K for annealed PPTA (Kevlar 49). [b] Under σ_t = 0.15 GPa. [c] Under σ = 0.114 GPa. [d] Estimated from the tensile curve by the present authors. [e] Northolt et al. reported extrapolated sonic moduli, 160 and 240 GPa.

Table III
Comparisons of Mechanical Properties between Lattice and Bulk for PBA

	$\Delta\epsilon/\Delta T \times 10^6$ [a]	$\Delta J/\Delta T \times 10^6$ [a]	J(RT) $\times 10^3$ [b]
unit	K^{-1}	$(GPa\cdot K)^{-1}$	GPa^{-1}
lattice	−6.7	7.0	5.3
tensile	−8.1	7.6	5.9
(t/l)[c]	1.2	1.1	1.1

[a] Average gradients between 300 and 600 K. [b] J(RT) is the compliance at room temperature (293 K) for the annealed state. [c] (t/l) is the tensile (bulk) value/lattice value.

ment with the theoretical estimation for the trans conformation listed in Table II.

Mechanical Models for PBA and PPTA Fibers. In Tables III and IV are summarized the thermal and mechanical properties measured for the bulk and the crystal lattice for the PBA and PPTA fibers, respectively. Notice here that the (macroscopic value)/(microscopic value) ratios for the thermal expansion coefficient, the compliance, and the temperature dependence of compliance are very close to unity over a wide temperature range for the PBA fiber. That is to say the behavior of the bulk is almost the same as that of the crystalline part in both the thermal and mechanical parameters for PBA. Thus a simple parallel model of crystalline and noncrystalline phases (or an almost ideal paracrystalline model) may be sufficient for the PBA fiber. On the other hand, for the PPTA fiber, the (macroscopic value)/(microscopic value) ratios are considerably larger than unity, about 1.5–2.5. In general, the elastic constant is appreciably sensitive to the slight structural change of the chain conformation or the defect contained in the sample. Therefore we may take the compliance J as a suitable index for the degree of the structural perfection along the fiber direction. The comparatively large difference in the compliance between the bulk (J_t = 8.9 × 10^{-3} GPa^{-1}) and the lattice (J_l = 6.0 × 10^{-3} GPa^{-1}) suggests that the population of the fully extended chains, which owes the tensile stress in the noncrystalline part, is not so high in the case of PPTA fiber; in other words, the structural regularity along the chain direction may not be so high in the paracrystalline state of PPTA compared with the case of PBA. Thus a suitable mechanical model of PPTA fiber may be rather close to the simple series model of the crystalline and noncrystalline phases. Such a consideration is consistent with the morphological studies of Kevlar and Kevlar 49 by Dobb et al.[29] and Panor et al.[30]

Table IV
Comparisons of Mechanical Properties between Lattice and Bulk for PPTA

	$\Delta\epsilon/\Delta T \times 10^6$ [a]	$\Delta J/\Delta T \times 10^6$ [b]	J(RT) $\times 10^3$ [c]
unit	K^{-1}	$(GPa\cdot K)^{-1}$	GPa^{-1}
lattice	−3.4	6.4	6.0
tensile	−6.7	9.4	8.9
(t/l)[c]	2.0	1.5	1.5

[a] Average gradients between 300 and 600 K. [b] J(RT) is the compliance at room temperature (293 K) for the annealed state. [c] (t/l) is the tensile (bulk) value/lattice value.

Registry No. PBA (SRU), 24991-08-0; PBA (homopolymer), 25136-77-0; PPTA (SRU), 24938-64-5; PPTA (copolymer), 25035-37-4.

References and Notes

(1) Morgan, P. W. *Macromolecules* **1977**, *10*, 1831.
(2) Kwolek, S. L.; Morgan, P. W.; Schaefgen, J. R.; Gulrich, L. W. *Macromolecules* **1977**, *10*, 1390.
(3) Kwolek, S. L. U.S. Patent 3 600 350, Aug 17, 1971; U.S. Patent 3 671 542, June 20, 1972.
(4) Blade, H. U.S. Patent 3 767 756, Oct 23, 1973.
(5) Bair, T. I. U.S. Patent 3 817 941, June 18, 1974.
(6) Tashiro, K.; Kobayashi, M.; Tadokoro, H. *Macromolecules* **1977**, *10*, 413.
(7) Gaymans, R. G.; Tijssen, J.; Harkama, S.; Bantjes, A. *Polymer* **1976**, *17*, 517.
(8) Slutsker, L. I.; Utevskii; L. E.; Chereiskii, Z. Yu.; Perepelkin, K. E. *J. Polym. Sci., Polym. Symp.* **1977**, *No. 58*, 339.
(9) Yabuki, K.; Ito, H.; Ota, T. *Sen'i Gakkaishi* **1975**, *31*, T-524. Yabuki, K.; Ito, H.; Ota, T. *Ibid.* **1976**, *32*, T-55. Yabuki, K.; Koda, H.; Endo, S.; Kagima, I.; Yukimatsu, K.; Konomi, T. *Ibid.* **1978**, *34*, T-342.
(10) Northolt, M. G.; Van Aartsen, J. J. *J. Polym. Sci., Polym. Symp.* **1977**, *No. 58*, 283. Northolt, M. G. *Polymer* **1980**, *21*, 1199. Northolt, M. G.; Hout, R. v. d. *Polymer* **1985**, *26*, 310.
(11) Wakelin, J. H.; Sutherland, A.; Beck, L. R., Jr. *J. Polym. Sci.* **1960**, *42*, 139.
(12) Davis, G. T.; Eby, R. K.; Colson, J. P. *J. Appl. Phys.* **1970**, *37*, 4316.
(13) Kobayashi, Y.; Keller, A. *Polymer* **1970**, *11*, 114.
(14) Chen, F. C.; Choy, C. L.; Young, K. *J. Polym. Sci., Polym. Phys. Ed.* **1980**, *18*, 2313.
(15) Ii, T.; Tashiro, K.; Kobayashi, M.; Tadokoro, H. *Macromolecules* **1986**, *19*, 1809.
(16) Ii, T.; Tashiro, K.; Kobayashi, M.; Tadokoro, H. *Macromolecules* **1986**, *19*, 1772.
(17) Clements, J.; Jakeways, R.; Ward, I. M. *Polymer* **1978**, *19*, 639.
(18) Miyasaka, K.; Isomoto, T.; Koganeya, H.; Uehara, K.; Ishikawa, K. *J. Polym. Sci., Polym. Phys. Ed.* **1980**, *18*, 1047.
(19) Nakamae, K.; Nishino, T.; Hata, K.; Matsumoto, T. *Polym. Prepr. Jpn.* **1983**, *32*, 2421; Meeting of the Society of Polymer Science, Japan, Kobe, 1984, p 39.
(20) Ii, T.; Tashiro, K.; Kobayashi, M.; Tadokoro, H., to be published.
(21) *Kevlar Aramide Data Manual*; Du Pont: Wilmington, DE, 1975.
(22) Hasegawa, R. K.; Chatani, Y.; Tadokoro, H. Meeting of the Crystallographic Society of Japan, Osaka, Japan, 1973, Preprints, p 21.
(23) Northolt, M. G.; Van Aartsen, J. J. *J. Polym. Sci., Polym. Lett. Ed.* **1973**, *11*, 333. Northolt, M. G.; Stuut, H. A. *J. Polym. Sci., Polym. Phys. Ed.* **1978**, *16*, 939.
(24) Sakurada, I.; Ito, T.; Nakamae, K. *J. Polym. Sci., Part C* **1966**, *15*, 75.
(25) Holliday, L.; White, J. W. *Pure Appl. Chem.* **1971**, *26*, 545.

(26) Fielding-Russell, G. S. *Text. Res. J.* **1971**, *41*, 860.
(27) Perepelkin, K. E.; Chereiskii, Z. Yu *Prepr. Int. Symp. Man-Made Fibers, Kalinin, USSR*, **1974**, *1*, 142 (cited in ref 8).
(28) Kaji, K.; Sakurada, I. Meeting of the Society of Polymer Science, Japan, Kobe, 1975, p 56.
(29) Dobb, M. G.; Johnson, D. J.; Saville, B. P. *J. Polym. Sci., Polym. Symp.* **1977**, *No. 58*, 237.
(30) Panor, M.; Abakian, P.; Blume, R. C.; Gardner, K. H.; Gierke, T. G.; Yang, H. H. *J. Polym. Sci., Polym. Phys. Ed.* **1983**, *21*, 1955.

Elastic Behavior of *cis*-1,4-Polybutadiene

R. W. Brotzman*‡ and P. J. Flory†

IBM Research Laboratory, San Jose, California 95193. *Received February 4, 1986*

ABSTRACT: This study presents uniaxial extension measurements on *cis*-1,4-polybutadiene networks of known junction functionality. The observed values of the reduced force from uniaxial extension measurements conform to the constrained junction theory of Flory. The reduced force intercept at $1/\alpha = 0$ is fully comprehensible in terms of the cycle rank of the network and can be calculated from chemical considerations. This holds even though the polybutadiene melt has a high-plateau modulus. Therefore, discrete topological entanglements do not contribute perceptibly to the equilibrium modulus of polybutadiene networks.

Introduction

The reduced stress in uniaxial extension is defined by

$$[f^*] = f^*(V/V^0)^{-1/3}(\alpha - \alpha^{-2})^{-1} \quad (1)$$

where f^* is the tensile force per unit area in the reference state, V^0 is the volume of the reference state, V is the system volume at measurement, and α is the extension ratio relative to the length of the sample when isotropic at the same volume V. The reduced force is a convenient measure of the elastic response of a polymer network to an applied stress. According to earlier theories, $[f^*]$ should be constant.[1] In fact, it generally decreases markedly with elongation. Recent theory reformulates $[f^*]$ of a real polymer network as[2-5]

$$[f^*] = [f_{ph}^*](1 + f_c/f_{ph}) \quad (2)$$

where f_{ph} represents the force which would be exerted by a topologically equivalent phantom network, f_c is the contribution of the force from the effects of constraints on the fluctuations of network junctions, and $[f_{ph}^*]$ is the reduced force for the equivalent phantom network (i.e., a hypothetical network devoid of material properties; its constituent chains can transect one another, no chain excludes others from the volume it occupies, and the fluctuations of cross-links are constrained only by the chains attached directly to it). The reduced force for a perfect phantom network is given, according to theory,[3,6] by

$$[f_{ph}^*] = \xi kT/V^0 = (\phi - 2)\mu_J/2V^0 \quad (3)$$

where ξ is the cycle rank of the network, μ_J the number of network junctions, and ϕ the junction functionality. The ratio f_c/f_{ph} depends on two parameters κ and ζ; κ is of primary importance and is defined as the ratio of the mean-square radius of the fluctuations of the junctions in the phantom network to the mean-square radius of the Gaussian domain of constraint in the undistorted network, while the secondary parameter ζ is empirical and may reflect inhomogeneities of the network topology. It is given by eq 43 in ref 4. In the limit of high extension and/or dilution, f_c/f_{ph} vanishes according to this theory.

Thus elastic behavior in the limit of high extension and/or dilution is fully comprehensible from a consideration of the covalent structure of the network. Equation 3 implicitly excludes contributions to the reduced force from discrete entanglements[3] of one network chain with another. If a contribution should be included for permanently "trapped entanglements" of this nature, as is often contended to be necessary, their contribution would be reflected in apparent values of ξ, or of μ_J, exceeding those deduced from the chemical constitution of the network alone. Some authors have attempted to ascribe such contributions to the plateau modulus of the un-cross-linked polymer melt.[7,8] Equilibrium swelling data provide additional confirmation of the relationship between the reduced force of a phantom network and the cycle rank density determined from chemical considerations. Theoretical treatment of swelling data in the phantom network limits yields[9-11]

$$(\xi/V^0) = -[\ln(1 - v_{2,s}) + v_{2,s} + \chi v_{2,s}^2](v_{2,s}^{-1/3}/V_1) \quad (4)$$

where $v_{2,s}$ is the volume fraction of polymer at swelling equilibrium, χ is the polymer–solvent interaction parameter, and V_1 is the molar volume of the diluent.

This study presents uniaxial extension measurements on *cis*-1,4-polybutadiene (PBD) networks of known junction functionality. Primary PBD chains were cross-linked by a hydrosilylation reaction between the PBD double bonds and 1,1,3,3,5,5,7,7-octamethyltetrasiloxane (OMTS)

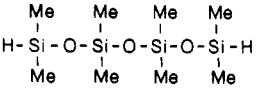

to produce a network that contains tetrafunctional junctions. The value of $[f_{ph}^*]$ determined from uniaxial extension measurements is compared with the stoichiometric value calculated from eq 3. The polybutadiene melt has a high-plateau modulus (1.2 MPa)[12] and thus provides a model system well suited for assessment of whether or not discrete topological entanglements contribute to the equilibrium modulus of an elastomer network.

Previous investigators have studied PBD networks formed by the action of free radicals induced photochemically, by peroxide, or by high-energy radiation. In a dicumyl peroxide charged system, Van der Hoff[13] estimated the cross-linking efficiency to be approximately 12 for each

† Deceased Sept 8, 1985.
‡ Present address: Department of Chemistry, CUNY, Staten Island, NY 10301.

0024-9297/87/2220-0351$01.50/0